

Material Behaviour

Rupture of swollen styrene butadiene rubber

Huiming Wang^{a,b}, Ken Wang^a, Wei Fan^c, Shengqiang Cai^{c,*}^a Department of Engineering Mechanics, Zhejiang University, Hangzhou, 310027, People's Republic of China^b Key Laboratory of Soft Machines and Smart Devices of Zhejiang Province, Zhejiang University, Hangzhou, 310027, People's Republic of China^c Department of Mechanical and Aerospace Engineering, University of California, San Diego, La Jolla, CA 92093, USA

ARTICLE INFO

Article history:

Received 1 April 2017

Accepted 13 May 2017

Available online 16 May 2017

Keywords:

Oil-swellaible elastomer

Fracture energy

Rupture

ABSTRACT

Elastomers have recently been explored to make swellable packers in the oil industry, which have many advantages over traditional cement packers. In the applications, the elastomers absorb solvent and swell against the confinement, which can seal zones in the borehole. In addition, swollen elastomers are usually subjected to a large pressure difference, which can cause fracture of the elastomer. In this article, we conduct experimental studies of the rupture behavior of an oil-swellaible elastomer, styrene butadiene rubber (SBR), swollen in hexadecane. This combination of elastomer and swelling agent can be considered representative of oilfield applications. Pure-shear tests are used to measure the stretch at rupture and fracture energy of swollen SBR with different swelling ratios. It is found that swelling can significantly reduce both the stretch at rupture and the fracture energy of the swollen elastomer. Using the measured fracture energy, we have also successfully predicted the stretches at rupture of SBR for a simple extension test with different volume swelling ratios.

© 2017 Elsevier Ltd. All rights reserved.

1. Introduction

Crosslinked elastomers can absorb solvent and swell. Recently, swellable elastomers have been widely explored in a myriad of engineering applications. For example, swelling elastomers have been developed as self-regulating valves in microfluidics [1–4]. Swellaible elastomers have also been explored to make swellable packers in the oil industry to replace traditional cement packers [5–8]. In these applications, swollen elastomers may rupture when the deformation is large with a sufficiently large flaw size in the material [9,10].

Although rupture of dry elastomers has been intensively studied over several decades [11–17], few systematic investigations of fracture in swollen elastomers have been conducted. It is known that the viscosity of an elastomer can be dramatically decreased by solvent-induced swelling which, consequently, can cause a reduction in the fracture energy of the elastomer. It has also been shown that threshold fracture energy of an elastomer can be measured in its swollen state with low strain rate and high temperature [15–17]. The measured threshold fracture energy of elastomers agrees

reasonably well with the predictions from classical Lake-Thomas theory [18]. Such agreement has provided important insights into the rupture of elastomers. Nevertheless, the rupture process of swollen elastomers in engineering applications usually greatly deviates from threshold conditions. Therefore, it is practically important to study rupture of swollen elastomer under various loading conditions and swelling ratios. Moreover, it is critical to verify if the fracture energy of swollen elastomer measured in one loading condition can be used as a material parameter to predict its rupture in other loading conditions.

In this article, we focused on the rupture of swellable elastomers used in oilfields. During the last decade, swelling of elastomers has been widely used in oilfield to seal the fluid flow in well bores [19–21]. Fracture in swollen elastomers has been recognized as one important failure mechanism for seals [10]. To study rupture of swollen elastomers, we carried out experiments on styrene butadiene rubber (SBR) swollen in hexadecane by following the “pure-shear” method first proposed by Rivlin and Thomas [14]. From these experiments, we found that both the fracture energy and the stretch at rupture decrease with increase of the degree of swelling and decrease of loading rate. Furthermore, using the measured fracture energy, we successfully predicted the stretch at rupture of elastomer for simple extension tests with different swelling ratios.

* Corresponding author.

E-mail address: shqcai@ucsd.edu (S. Cai).

2. Experiments

An oil-swellaible elastomer, styrene butadiene rubber (SBR) (purchased from the website: <http://www.rubbersheetroll.com/sbr-commercial-grade.htm>), was used to swell in hexadecane at room temperature of about 20 °C. Following our previous work [6], this combination of elastomer and swelling agent can be considered representative of oilfield applications.

2.1. Preparation of SBR sheets with different swelling ratios

In the swelling experiments, a dry SBR sheet with length $L = 60$ mm, height $H = 6$ mm and thickness $B = 1.5$ mm was immersed in hexadecane. The length, width and thickness of the swollen sample were measured at different times until it reached equilibrium state. The weight of the swollen sample was also measured at the same time. We then calculated the volume swelling ratio (VSR) and weight swelling ratio (WSR), which are defined as the ratio between the increase of the volume/weight and the initial volume/weight of the dry SBR sheet, respectively. Fig. 1(a) and (b) plot VSR and WSR as a function of time, respectively. It can be seen that the sample reached equilibrium state within 40 h.

To prepare SBR sheets with different swelling ratios, we immersed the sheets in solvent for different periods of time. Then, the swollen sheets were removed from the solvent and sealed in soft impermeable plastic films for 24 h for homogenization. It is noted that the weight of swollen sheets measured before and after the application of the impermeable films ensured that no evaporation occurred during homogenization. For tests with a pre-cut, a 10 mm long pre-cut was introduced freshly by using a sharp knife after the sample was homogenized.

2.2. Measurement of fracture energy of swollen SBR sheets

We adopted pure-shear tests to measure fracture energy of swollen SBR sheets. The tests were carried out in a mechanical testing machine (Zwick/Z010). During the test, to avoid possible slip of the samples in the grips, SBR sheets were firmly glued to two acrylic plates. Then, the acrylic plates were firmly clamped in the testing machine. During the test, the samples were stretched in the direction along its height at a constant extension rate. In our experiments, three extension rates were selected as 0.2/min, 2/min, and 20/min. It is noted that these extension rates were defined relative to the initial height of the sample. For instance, if the initial height of the specimen was $H = 6$ mm and the extension rate was 2/min, the stretching speed was then set to be 12 mm/min. The tensile force and displacement were recorded automatically by the testing machine. Tests were made in triplicate.

Fig. 2 is the photographs of dry SBR specimen during a “pure-shear” test. Fig. 2(a) shows the undeformed state of a pristine sample. During the extension test of the pristine sample, an arch-shaped edge was observed when the stretch was relatively large (Fig. 2(b)). Eventually, the specimen ruptured (Fig. 2(c)).

The undeformed state of the specimen with a pre-cut is shown in Fig. 2(d). During the test of the specimen with a pre-cut, with the increase of stretch, the crack-tip was first blunted, as shown in Fig. 2(e). At a certain stretch, the crack started to propagate, as shown in Fig. 2(f). The critical point at which the crack started to propagate can be clearly seen with the naked eye. The stretch corresponding to this critical point is defined as the stretch at rupture [22].

Figs. 3 and 4 show the nominal stress-stretch curves for the specimens without and with a pre-cut. The specimens were swollen in hexadecane with different volume swelling ratios, 0.0%

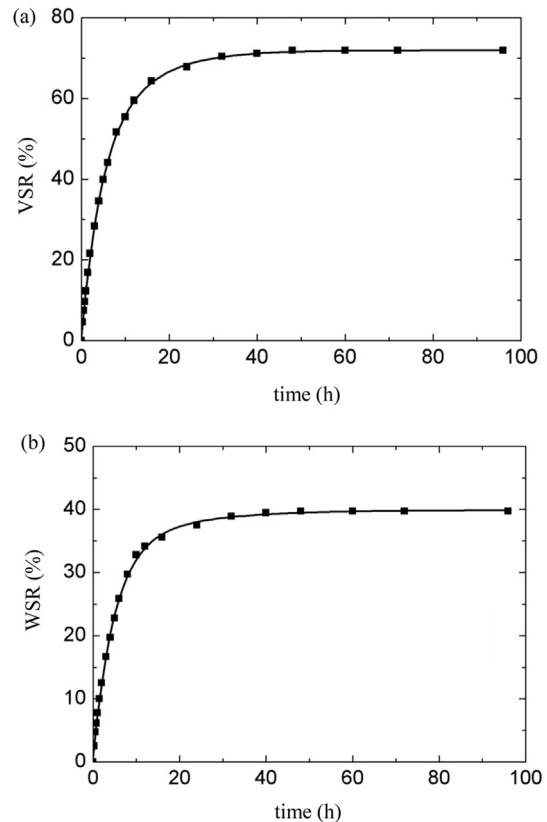


Fig. 1. Experimental measurements of swelling ratio of SBR in hexadecane as function of time. (a) Volume swelling ratio (VSR) as a function of time. VSR is defined as the ratio between the increase of volume and the initial volume of an SBR sample. (b) Weight swelling ratio (WSR) as a function of time. WSR is defined as the ratio between the increase of weight and the initial weight of an SBR sample.

(dry state), 12.3% (swollen in hexadecane for 1 h), 33.9% (swollen in hexadecane for 5 h) and 71.8% (fully swollen state). Three stretch rates 0.2/min, 2/min and 20/min were adopted in the pure-shear test.

Based on the “pure-shear” test, the fracture energy I of the SBR sheet can be calculated as

$$\tau = W(\lambda_{rup}) \cdot H \quad (1)$$

where H is the height of the specimen in the undeformed state and $W(\lambda_{rup})$ is the area under the nominal stress-stretch curve of a specimen without a pre-cut between 1.0 to λ_{rup} . Here λ_{rup} is the stretch at rupture of the pre-cut specimen.

2.3. Simple extension of SBR sheets with edge crack

Simple extension tests of SBR sheets were also carried out in the same mechanical testing machine (Zwick/Z010). The stretch rate in the simple tension test was set as 2/min. The geometry of the sample was taken as: length: $L = 100$ mm (in loading direction) and width: $H = 20$ mm. Simple extension tests were performed for SBR samples with four different volume swelling ratios which were VSR = 0.0%, 12.3%, 33.9% and 71.8%. To compare the theoretical predictions with the experimental measurements in the simple extension test, pre-cuts of four different lengths were introduced into the samples, which were $c = 1.5$ mm, 2.5 mm, 5 mm and 8 mm. It is noted that pre-cuts were also introduced freshly in the sample just before the mechanical tests.

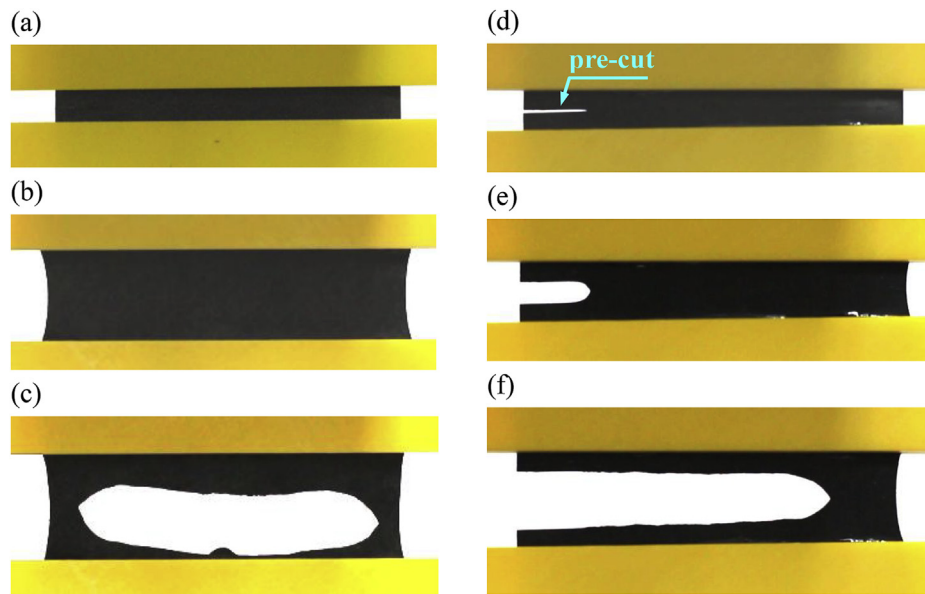


Fig. 2. Photographs of SBR sheet under pure shear test. (a) Pristine SBR sheet in the undeformed state. The thickness, height and width of the sheet are 1.5 mm, 6 mm and 60 mm, respectively. (b) Pristine SBR sheet in stretched state. (c) Rupture of pristine SBR sheet when the stretch is too large. (d) Undeformed SBR sheet with a pre-cut of 10 mm long. (e) Stretched SBR sheet with a pre-cut. Crack tip gets blunted with the stretch. (f) When the stretch reaches a critical value, crack begins to propagate.

3. Results and discussions

3.1. Stretch at rupture

Under pure-shear loading, the stretch at rupture for both pristine samples and the samples with a pre-cut for different VSRs are shown in Fig. 5. For both pristine samples and the samples with a pre-cut, for a fixed stretch rate, the stretch at rupture λ_{rup} was reduced by increasing the volume swelling ratio. For instance, for a stretch rate of 20/min, the stretch at rupture for pristine samples was 3.055 ± 0.045 for VSR = 0% (dry state), 2.683 ± 0.066 for VSR = 12.3%, 2.124 ± 0.042 for VSR = 39.9% and 1.646 ± 0.026 for VSR = 71.8% (fully swollen state). At a stretch rate of 0.2/min, the stretch at rupture for the samples with a pre-cut was 1.546 ± 0.023 for VSR = 0% (dry state), 1.431 ± 0.047 for VSR = 12.3%, 1.327 ± 0.018 for VSR = 39.9% and 1.262 ± 0.015 for VSR = 71.8% (fully swollen state). The symbol “ \pm ” here indicates standard deviation.

3.2. Fracture energy of swollen SBR

Fracture energy of SBR is plotted in Fig. 6 as a function of VSR at different stretch rates. The experimental results show that, at the same stretch rate, the fracture energy can significantly decrease with increase of VSR. For example, for a stretch rate of 2/min, fracture energy of SBR was decreased from 4235.5 ± 569.9 J/m² for VSR = 0% (dry state), to 457.2 ± 16.7 J/m² for VSR = 71.8% (fully swollen state). For a fixed swelling ratio, fracture energy of SBR also decreases with the decrease of stretch rate. For instance, for VSR = 39.9%, fracture energy of SBR decreases from 1232.2 ± 241.7 J/m² for a stretch rate of 20/min to 769.7 ± 72.3 J/m² for a stretch rate of 0.2/min.

Fracture energy of a swollen elastomer mainly has contributions from the elastic energy stored in broken polymer chains, viscous damping from polymer network and migration of solvent in the elastomer during rupture. The dissipated elastic energy stored in broken polymer chains during rupture can be defined as threshold fracture energy [17,18], which is estimated to be around 20 J/m² and is typically regarded as an intrinsic material property. In fact, to

measure threshold fracture energy of rubber, researchers often conducted fracture tests of rubber at high temperature, low strain rate and in a swollen state. Threshold fracture energy of rubber was estimated from breaking polymer chains, which can be regarded as the minimum fracture energy of rubber in arbitrary loading conditions. In our tests, the fracture energy of SBR dramatically decreases from 5200 J/m² for the highest stretch rate and dry condition to 400 J/m² for the lowest stretch rate and largest swelling ratio, which are significantly higher than estimated threshold fracture energy. This indicates that, in all our tests, the viscoelasticity of polymer network and migration of solvent may have important contributions to the measured fracture energy. With the increase of swelling ratio, the effective crosslinking density of the rubber decreases. In addition, swelling can dramatically reduce viscosity of the rubber. As a consequence, fracture energy of the rubber decreases with increasing swelling ratio. To make the above measurements useful, it is imperative to check if it is possible to use the measured fracture energy, as shown in Fig. 6, to predict rupture of swollen SBR sheets subjected to other loading conditions.

3.3. Predictions of rupture of swollen SBR sheets under simple extension

We next used the measured fracture energy of swollen SBR to predict its rupture when subjected to simple extension. Based on scaling analysis, the stretch at rupture for a rubber sheet with an edge crack with length c under simple extension can be predicted using the following equation [23],

$$c = \frac{\tau}{2k(\lambda_{rup})W(\lambda_{rup})} \quad (2)$$

In the above equation, τ is the fracture energy of the elastomer, $k(\lambda)$ is taken the form following [23],

$$k(\lambda) = \frac{2.95 - 0.08(\lambda - 1)}{\sqrt{\lambda}} \quad (3)$$

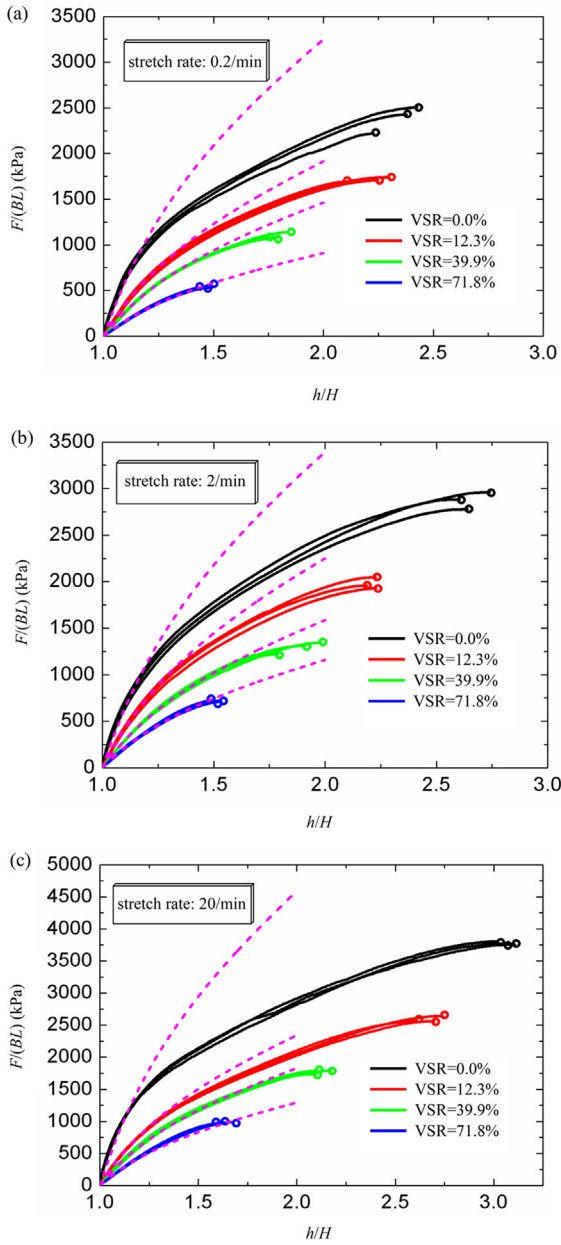


Fig. 3. Stress-stretch curves of pristine SBR samples with different swelling ratios and stretch rates. The stretch rates are (a) 0.2/min, (b) 2/min and (c) 20/min. The dashed lines are the fitting curves given by the neo-Hookean model.

and $W(\lambda)$ is strain energy density of the elastomer with stretch λ . For the neo-Hookean model, strain energy function $W(\lambda)$ for simple extension can be given by:

$$W(\lambda) = \frac{1}{2} \mu (\lambda^2 + 2\lambda^{-1} - 3) \quad (4)$$

where μ is the shear modulus of the elastomer. We obtained shear modulus of SBR with different VSRs by fitting the stress-strain relations for pure-shear loading condition predicted by the neo-Hookean model and measured in experiments, as shown in Fig. 3. Subjected to pure-shear load, nominal stress and stretch for a neo-Hookean solid is given by,

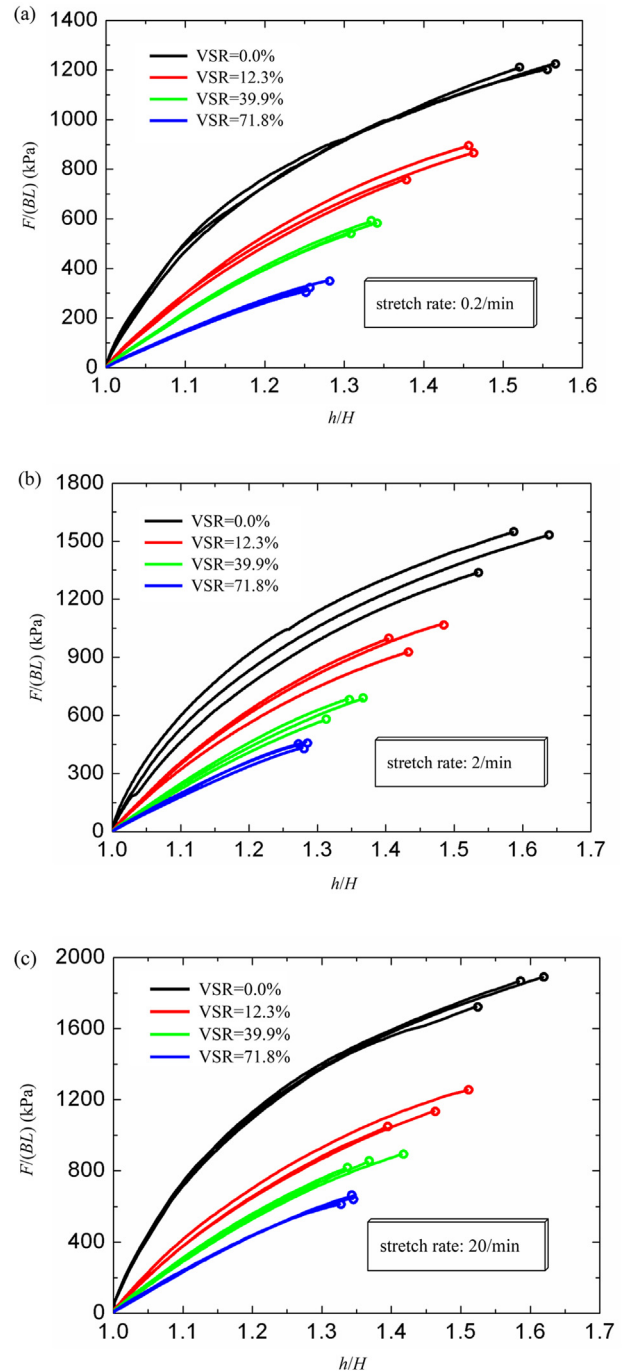


Fig. 4. Stress-stretch curves of SBR samples containing a pre-cut with different swelling ratios and stretch rates. The stretch rates are (a) 0.2/min, (b) 2/min and (c) 20/min.

$$s(\lambda) = \mu (\lambda - \lambda^{-3}) \quad (5)$$

Fig. 7 shows the fitted shear modulus of SBR as a function of swelling ratio under different stretch rates. When stretch is smaller than 1.5, the agreements between the measurements and predictions given by Eq. (5) are reasonably good. When stretch is large, we can see clear discrepancy between the predictions and measurements, which is mainly due to the limitation of the neo-Hookean model itself and ignoring viscoelasticity in the model.

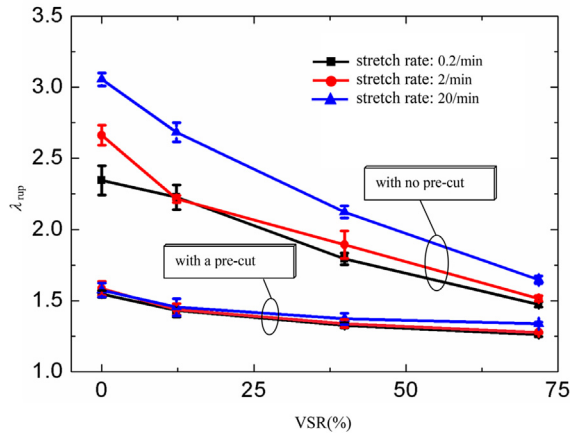


Fig. 5. Stretch at rupture of SBR sheets for different swelling ratios and stretch rates.

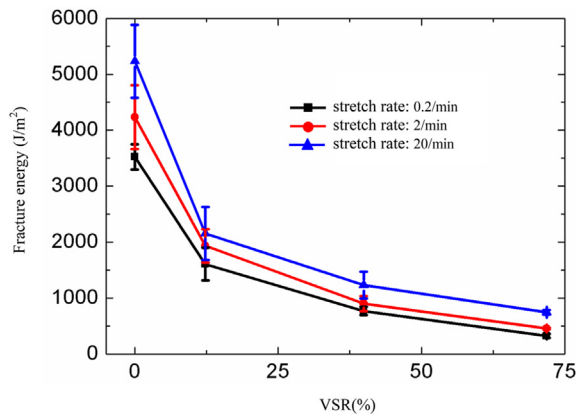


Fig. 6. Fracture energy of SBR for different swelling ratios and stretch rates.

In the current study, we regard neo-Hookean model as a phenomenological constitutive model. Although there are many other hyperelastic models available, most of those models reduce to neo-Hookean model when the deformation in the material is not too large. Despite of the disagreement between the prediction from neo-Hookean model and our measurement with large deformation, we still adopted the neo-Hookean model to predict the stretch at rupture of SBR under simple extension tests, because

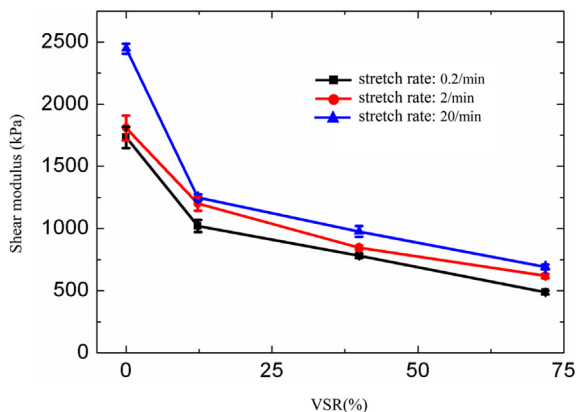


Fig. 7. Fitted shear modulus of SBR as a function of swelling ratio at different stretch rates.

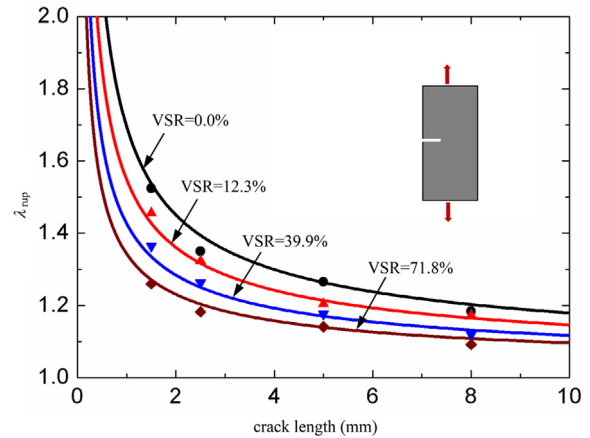


Fig. 8. Comparisons between the predictions and experimental measurements of stretch at rupture of swollen SBR sheets with an edge crack subjected to simple extension as shown in the inset. The stretch rate for the simple extension is fixed as 2/min. In the figure, solid lines are theoretical predictions and discrete dots are experimental data.

the stretch at rupture in most measurements, as shown in Fig. 8, was lower than 1.5.

Using the shear modulus fitted from the pure-shear test with stretch rate of 2/min and Eq. (2), we predicted the stretch at rupture for swollen SBR subjected to simple extension and with an edge crack of different lengths. The comparison between our predictions and measurements are shown in Fig. 8. The good agreement between the predictions and measurements implies that the fracture energy of swollen SBR measured in pure-shear loading can, indeed, be regarded as material parameter, which is independent of sample geometry.

4. Conclusions

We conducted systematic experimental studies of rupture behavior of oil-swellable elastomer, SBR, swollen in hexadecane with different volume swelling ratios. We found that both the stretch at rupture and fracture energy of SBR can be significantly reduced by either increasing its swelling ratio or decreasing the stretch rate. We believe such effects are mainly due to the viscoelasticity of SBR. We have further shown that, using the measured fracture energy and shear modulus of SBR specimen under pure-shear load, we can successfully predict the stretch of rupture of swollen SBR with an edge crack of different lengths and under simple extension. Therefore, fracture energy of swollen SBR measured under pure-shear load can be regarded as a material parameter, which is independent of the sample geometry.

Acknowledgements

H. Wang acknowledges the support from the National Natural Science Foundation of China [grant numbers 11372273 and 11621062]. S. Cai acknowledges the support from American Chemical Society through Award [grant number 55379-DNI9].

References

- [1] D.J. Beebe, J.S. Moore, J.M. Bauer, Q. Yu, R.H. Liu, C. Devadoss, B.H. Jo, Functional hydrogel structures for autonomous flow control inside microfluidic channels, *Nature* 404 (6) (2000) 588–590.
- [2] J.t. Schiphorst, S. Coleman, J.E. Stumpel, A.B. Azouz, D. Diamond, A.P.H.J. Schenning, Molecular design of light-responsive hydrogels, for in situ generation of fast and reversible valves for microfluidic applications, *Chem. Mater* 27 (17) (2015) 5925–5931.

- [3] X.Q. Zhang, L.J. Li, C.X. Luo, Gel integration for microfluidic applications, *Lab. Chip* 16 (2016) 1757–1776.
- [4] L. Dong, H.R. Jiang, Autonomous microfluidics with stimuli-responsive hydrogels, *Soft Matter* 3 (2007) 1223–1230.
- [5] M. Akhtar, S.Z. Qamar, T. Pervez, Swelling elastomer applications in oil and gas industry, *J. Trends Dev. Mach. Assoc. Technol.* 16 (1) (2012) 71–74.
- [6] Y. Lou, A. Robisson, S.Q. Cai, Z.G. Suo, Swellable elastomers under constraint, *J. Appl. Phys.* 112 (2012) 034906.
- [7] S.Z. Qamar, M. Akhtar, T. Pervez, M.S.M. Al-Kharusi, Mechanical and structural behavior of a swelling elastomer under compressive loading, *Mater. Des.* 45 (2013) 487–496.
- [8] M. Akhtar, S.Z. Qamar, T. Pervez, F.K. Al-Jahwari, FEM simulation of swelling elastomer seals in downhole applications, *Proceedings of the ASME 2013 International Mechanical Engineering Congress and Exposition (IMECE2013)*, San Diego, California, USA, 15–21 November, 2013.
- [9] R. Schirrer, P. Thepin, G. Torres, Water absorption, swelling, rupture and salt release in salt-silicone rubber compounds, *J. Mater. Sci.* 27 (1992) 3424–3434.
- [10] Z.J. Wang, C. Chen, Q.H. Liu, Y.C. Lou, Z.G. Suo, Extrusion, slide, and rupture of an elastomeric seal, *J. Mech. Phys. Solids* 99 (2017) 289–303.
- [11] W.V. Mars, A. Fatemi, A literature survey on fatigue analysis approaches for rubber, *Int. J. Fatigue* 24 (2002) 949–961.
- [12] C. Creton, M. Ciccotti, Fracture and adhesion of soft materials: a review, *Rep. Prog. Phys.* 79 (2016) 046601.
- [13] V. Lefèvre, K. Ravi-Chandar, O. Lopez-Pamies, Cavitation in rubber: an elastic instability or a fracture phenomenon? *Int. J. Fract.* 192 (2015) 1–23.
- [14] R.S. Rivlin, A.G. Thomas, Rupture of rubber. I. characteristic energy for tearing, *J. Polym. Sci.* 10 (1953) 291–318.
- [15] A.N. Gent, R.H. Tobias, Threshold tear strength of elastomers, *J. Polym. Sci. B, Polym. Phys.* 20 (1982) 2051–2058.
- [16] A.K. Bhowmick, A.N. Gent, C.T.R. Pulford, Tear strength of elastomers under threshold conditions, *Rubber Chem. Technol.* 56 (1983) 226–232.
- [17] A. Ahagon, A.N. Gent, Threshold fracture energies for elastomers, *J. Polym. Sci. B, Polym. Phys.* 13 (1975) 1903–1911.
- [18] G.J. Lake, A.G. Thomas, The strength of highly elastic materials, *Proc. R. Soc. Lond. A, Math. Phys. Sci.* 300 (1967) 108–119.
- [19] S.Q. Cai, Y. Lou, P. Ganguly, A. Robisson, Z.G. Suo, Force generated by a swelling elastomer subject to constraint, *J. Appl. Phys.* 107 (2010) 103535.
- [20] M. Akhtar, S.Z. Qamar, T. Pervez, R. Khan, M.S.M. Al-Kharusi, Elastomer seals in cold expansion of petroleum tubulars: comparison of material models, *Mater. Manuf. Process* 27 (2012) 715–720.
- [21] S.Z. Qamar, T. Pervez, M. Akhtar, M.S.M. Al-Kharusi, Design and manufacture of swell packers: influence of material behavior, *Mater. Manuf. Process* 27 (2012) 721–726.
- [22] M. Pharr, J.Y. Sun, Z.G. Suo, Rupture of a highly stretchable acrylic dielectric elastomer, *J. Appl. Phys.* 111 (2012) 104114.
- [23] P.B. Lindley, Energy for crack growth in model rubber components, *J. Strain Anal.* 7 (2) (1972) 132–140.